ORIGINAL PAPER

Thermal-hydraulic-mechanical coupling behavior and frost heave mitigation in freezing soil

Yukun Ji[1,2] · Guoqing Zhou[1] · Veerle Vandeginste[2,3] · Yang Zhou[1]

Abstract

Frost heave induced by artificial freezing can be destructive to infrastructure. The fundamental physicochemical mechanisms behind frost heave involve mainly the coupled thermal-hydraulic-mechanical (THM) behavior, ice-water phase transition, and heat and fluid flow in porous media. Taking the soil skeleton, pore ice, and pore water as independent bodies to conduct the mechanical analysis, we clarify the physical meaning of the effective stress principle of frozen soil with consideration of the multiphase interactions (ice-water-mineral) and further improve the coupled heat and fluid flow equations. Taking into account the coupled THM mechanism in freezing soils, a discrete ice lenses based model for frost heave is established with focus on segregation and growth of the ice lens. Upon validation of the frost heave model, an intermittent freezing method is applied to investigate mitigation of frost heave. Numerical results show that the intermittent freezing can significantly mitigate frost heave and inhibit the potential frost susceptibility of freezing soil. Our research reveals that the narrowing of the frozen fringe induced by the upward movement of the freezing front is the main reason for the slower growth of the ice lens. The THM behavior and heat and fluid flow based frost heave model enable a better understanding of the geomechanical properties of freezing soil and physical mechanism of frost heave mitigation in porous media (soil).

Keywords THM behaviors · Multiphase interactions · Heat and fluid flow · Frost heave model · Frost heave mitigation

Introduction

With the modernization of the cities and the need for economic development, the freezing method plays an important role in the construction of tunnels and metros due to its reliable performance for water proofing and strengthening soil (Hu and Deng 2016). The Hong Kong-Zhuhai-Macao Bridge, the world's longest sea-crossing bridge (55 km) in China consisting of an undersea tunnel (6.7 km) and four artificial islands, was officially opened to traffic in October 2018. The Freeze-Sealing Pipe Roof (FSPR) method has been successfully applied in the most technically demanding construction of the Gongbei tunnel, and the innovative thermal technology and experience in the construction of the undersea tunnel greatly encourage scholars and engineers to carry out further research and exploration on freezing theory and technology (Hu et al. 2017; Hu et al. 2018a, 2018b). Despite the merits of artificial ground freezing, there remain still some theoretical and technical challenges with the application of artificial ground freezing. The upward movement of surface caused by ice lens growth will affect the integrity of the infrastructures. Therefore, frost heave and frost heave mitigation are important research topics that have provoked great interest from researchers (Zhou 1999; Hu et al. 2018a, 2018b; Wang et al. 2018; Zhao et al. 2019; Zhang et al. 2019; Zhao et al. 2020), and a better understanding of the mechanism of frost heave mitigation still needs to be developed.

The ice-water thermodynamics behavior, multiphase interactions (ice-water-mineral), heat and fluid transport, and ice lens growth are involved in the main physical processes during freezing of a fine-grained porous media, which are the fundamental research in the field of the freezing soils (Zhang et al. 2016; Zhang et al. 2017; Li et al. 2018; Ji et al.

✉ Guoqing Zhou
gdue.zhou@gmail.com

1 State Key Laboratory for Geomechanics and Deep Underground Engineering, China University of Mining and Technology, Xuzhou 221116, Jiangsu, China

2 School of Chemistry, University of Nottingham, Nottingham NG7 2RD, UK

3 GeoEnergy Research Centre, Faculty of Engineering, University of Nottingham, Nottingham NG7 2RD, UK

2019). During freezing, the supercooled pore water (Dash et al. 1995) forms seepage conduits in porous media allowing the migration of external water to the freezing front via cryogenic suction induced by ice-water phase transition, which facilitates the macroscopic growth of soil-free ice lenses, resulting in frost heave. It should be noted that the study of the frost heave theoretical model provides not only a method for frost heave prediction, but it is also fundamental in our understanding of the coupled THM processes in freezing soil. An effective way to investigate frost heave mitigation may be introduced by the theory of water migration and ice lens growth under THM coupling scenario to reveal the ice lens growth controlling mechanism. The corresponding frost heave model research will provide valuable theoretical guidance for implementation of engineering construction in cold regions.

In contrast to the capillary theory (Everett 1961) which only depicts the growth of a single ice lens and underestimates frost heave pressures, Miller (1972) proposed frozen fringe theory (secondary frost heave) and indicated that the stable ice particles are formed in the pores at the bottom of the warmest ice lens. Moreover, the distinctive zone between the freezing front and the ice lens is referred to as the frozen fringe, and it is characterized with low fluid permeability and low water content. Subsequently, many researchers applied the frozen fringe theory as a basis to establish the frost heave model and successfully predicted the discrete ice lenses in freezing soils (Gilpin 1980; Nixon 1991; Rempel 2007; Bronfenbrener and Bronfenbrener 2010; Lai et al. 2014; Sheng et al. 2014; Zhou et al. 2018; Ji et al. 2018). Given the importance of the real THM coupling environment for discrete ice lens growth, we particularly need to understand the heat and fluid transport in the porous media during freezing. Additionally, the ice-water transition behavior during ice crystallization does not only cause pore blocking and slow down the flow rate of water migration, but it also affects the thermophysical properties of the porous media which play an important role in determining the heat and fluid transport (Hansson et al. 2004; Lackner et al. 2005; Lyu et al. 2019). The fluid permeability of partially frozen media is essentially determined by the soil freezing characteristics curve (SFCC), representing the relationship between unfrozen water content and suction or temperature, and it is an analog to the soil water characteristics curve (SWCC) (Koopmans and Miller 1966; Spaans and Baker 1996; Azmatch et al. 2012a, 2012b). Ice and water coexist in pores, and the mechanical behavior of the partially frozen porous media under multiphase interactions is similar to unfrozen and unsaturated media with replacement of pore water by ice crystals (except the ice-water phase transition) (Black and Tice 1989). A reasonable effective stress principle of frozen soil will benefit the development of the fully THM coupled equations with considering the stress development and ice-water phase transition in porous media.

According to analogy with the effective stress analysis of unsaturated soils (Shao et al. 2014; Shao et al. 2017), we have clarified the physical meaning of the effective stress principle of frozen soil and subsequently improved the governing equations of heat and fluid flow. Considering the coupled THM interactions in freezing soils, a discrete ice lenses based model for frost heave is established and developed under the corresponding physical and mechanical criterion. After a quantitative validation of this frost heave model, a frost heave model dependent intermittent freezing method is applied to investigate frost heave mitigation, and numerical simulation shows that intermittent freezing can indeed mitigate frost heave. Moreover, the numerical result demonstrates that the narrowing of the frozen fringe will decrease the growth rate of the ice lens and thus result in frost heave mitigation.

Effective stress of frozen soil

The continuum mechanics method is used to analyze the stress equilibrium of multiphase and porous frozen soil and to derive the equilibrium differential equation of each phase of the frozen soil. By comparing the equilibrium differential equation of soil skeleton stress with the equilibrium differential equation of total stress of the frozen soil, the effective stress of frozen soil which has an explicitly physical meaning is given and determined. The classical equilibrium differential equations of total stress of the frozen soil (ice-water-mineral coexistence system) are given in a Cartesian coordinate system:

$$\begin{cases} \dfrac{\partial \sigma_{tx}}{\partial x} + \dfrac{\partial \tau_{xz}}{\partial z} + X_{swx} = 0 \\ \dfrac{\partial \tau_{xz}}{\partial x} + \dfrac{\partial \sigma_{tz}}{\partial z} + X_{swz} = 0 \end{cases} \tag{1}$$

where σ_{tx}, σ_{tz}, and τ_{zx} are, respectively, the orthogonal normal stresses and the shear stress; X_{swx} and X_{swz} represent the specific weight of the soil mixture; and $X_{swx} = 0$ and $X_{swz} = \gamma_m$, γ_m stand for weight of frozen soil in the z-direction.

By selecting a representative element volume of saturated soil, Shao et al. (2014) separately take the soil skeleton and pore water as independent free bodies to study the effective stress, and they point out that the pore water pressure generates the surface force and the flow of pore water exerts the seepage force on the skeleton (Fig. 1a and b). Similarly, we selected ice, water, and matrix skeleton as independent bodies to conduct mechanical analysis of frozen soil and subsequently defined the effective stress of frozen soil in this paper. In order to clearly present the definition of effective stress of frozen soil, some basic results of Shao et al.'s theory (Shao et al. 2014; Shao et al. 2017) are introduced first. When the pore water in the granular media is removed, the effect of pore water pressure on soil skeleton will be extracted (Fig. 1b). Moreover, the pore water pressure exerted on the cross section
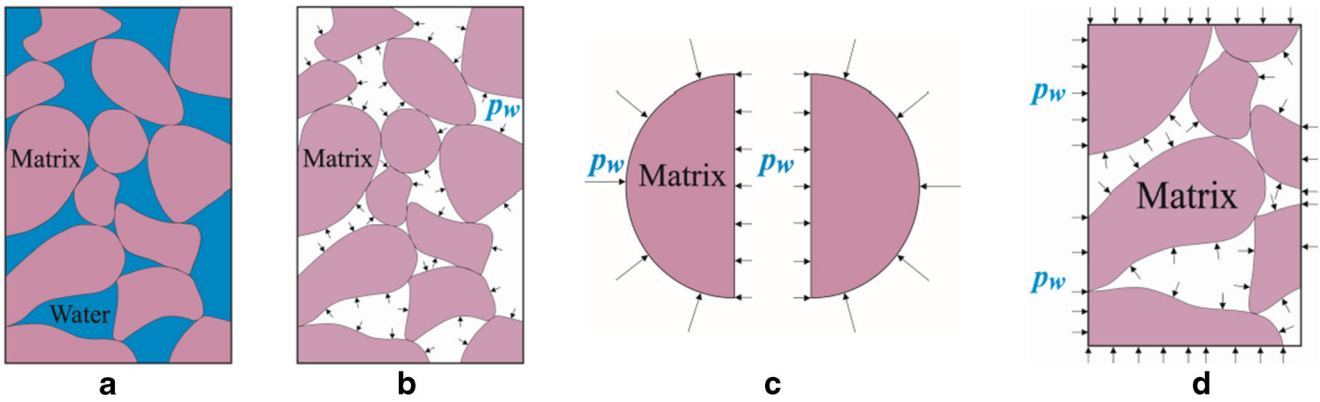
Fig. 1 Soil skeleton stress induced by pore fluid pressure (Shao et al. 2014; Shao et al. 2017): (**a**) Saturated soil (**b**) Effect of pore water pressure on soil skeleton (**c**) Particle stress on cross section (**d**) Pore water pressure on the cross section of the soil skeleton

of the soil skeleton (Fig. 1d) is the same as the average internal pressure of the particle caused by the pore water pressure (Fig. 1c). Therefore, the area where pore water pressure acts upon is the area of the soil skeleton. Furthermore, the internal force of the soil skeleton induced by pore water pressure is the product of the pore water pressure p_w and the soil skeleton area, i.e., $p_w(1 - n)A_n$, where n is porosity and A_n is the total area of soil.

In addition, the skeleton stress is the normal stress and shear internal stress generated by all external stresses excluding pore water pressure that acts upon the total area of the soil body, which are represented by $\sigma = N/A_n$ and $\tau = S/A_n$, where N and S represent normal and shear internal force (Shao et al. 2014). By using the similar method, Shao et al. (2014, 2017) separately take soil skeleton, pore water, and pore air as independent free bodies to study the effective stress of unsaturated soil. Actually, the freezing phenomenon in frozen soil and drying phenomenon in unfrozen soil are strikingly similar, during drying; the replacement of pore water by air results in a lower matrix potential; similar processes also occur in freezing soils with replacement of pore water by ice (Spaans and Baker 1996). The matrix suction that prevents the evaporation of water also inhibits the freezing of water (Spaans and Baker 1996). Hence, the matrix suction and ice (air) pressure influenced mechanical analysis are similar in both frozen media and that of the unfrozen unsaturated media. Based on the similarities between the SFCC and SWCC, Azmatch et al. (2012a, 2012b) evaluated the temperature conditions of ice lens segregation in the frozen fringe and the hydraulic permeability of partially frozen soil, and the observed consistency demonstrates the validity of this analogous method. The surface tension formed at the matrix-pore water interface inside the frozen soil is regarded as the interaction force between the soil skeleton and the pore water (body force). Similarly, the surface stress of the soil skeleton (Fig. 2) is presented according to analogy with the analysis of unsaturated soil (Shao et al. 2014). Based on the analysis above, the area where pore ice and pore water act upon is the soil skeleton area, $(1 - n)A_n$. Therefore, the corresponding proportions of each phase are $(1$

$- n)A_n\theta_i/n$ and $(1 - n)A_n\theta_w/n$, respectively (Fig. 2). Moreover, θ_i and θ_w stand for volumetric content of pore ice and pore water, and the relationship between volumetric content of pore ice and pore water is determined with consideration of a saturated frozen soil:

$$\theta_w + \theta_i = n \tag{2}$$

We take the soil skeleton, pore water, and pore ice as independent free bodies to carry out the mechanical equilibrium analysis (Fig. 3). p_i and p_w represent pore ice pressure and pore water pressure, respectively; σ_x, σ_z, τ_{xz}, and τ_{zx} are, respectively, orthogonal normal stresses and the shear stress of soil skeleton; and $f_{six}, f_{isx}, f_{siz}$, and f_{isz} stand for the interaction force (body force) between soil skeleton and pore ice in x-direction and z-direction with a same value but opposite direction; similarly, the interaction force between soil skeleton and pore water are $f_{swx}, f_{wsx}, f_{swz}$, and f_{wsz}; γ_d, γ_i, and γ_w are the specific weight of the soil, ice, and water.
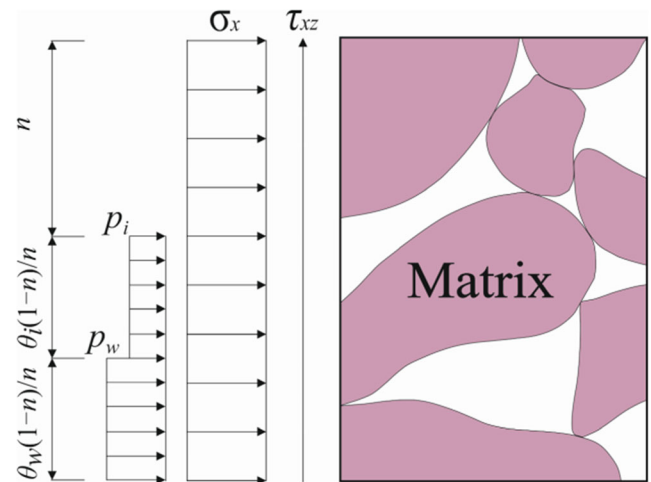
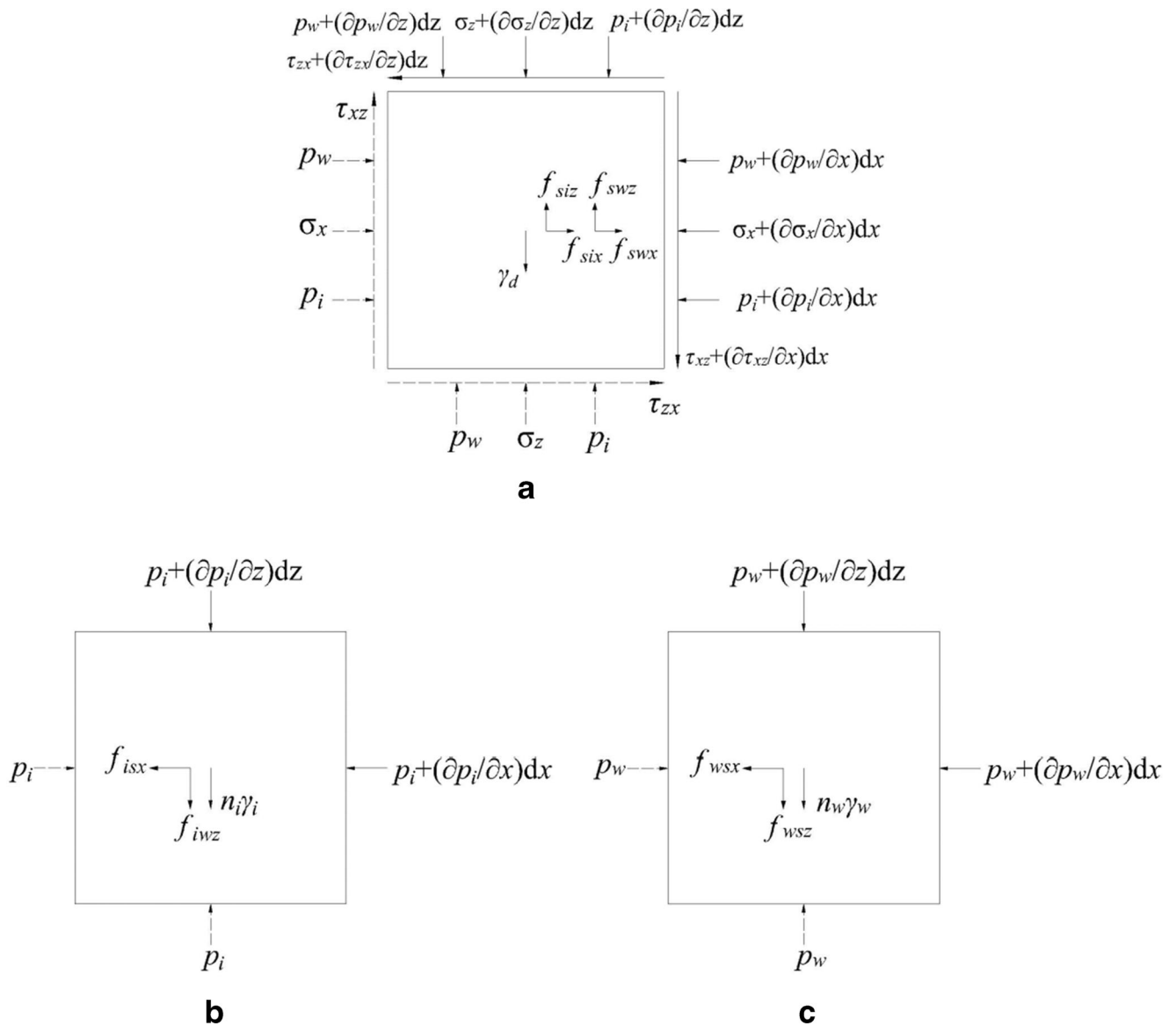**Fig. 2** Schematic of the surface stress of the soil skeleton in the x-direction

Fig. 3 Stress analysis of the soil skeleton, pore ice and pore water for frozen soil: (**a**) Skeleton of frozen soil (**b**) Pore ice (**c**) Pore water

The equilibrium differential equations of soil skeleton can be written as (Fig. 3a):

$$\begin{cases} \dfrac{\partial \sigma_x}{\partial x} + \dfrac{\partial \tau_{zx}}{\partial z} + \dfrac{1-n}{n}\dfrac{\partial(\theta_w p_w)}{\partial x} + \dfrac{1-n}{n}\dfrac{\partial(\theta_i p_i)}{\partial x} - f_{six} - f_{swx} = 0 \\ \dfrac{\partial \tau_{xz}}{\partial x} + \dfrac{\partial \sigma_z}{\partial z} + \dfrac{1-n}{n}\dfrac{\partial(\theta_w p_w)}{\partial z} + \dfrac{1-n}{n}\dfrac{\partial(\theta_i p_i)}{\partial z} - f_{siz} - f_{swz} + \gamma_d = 0 \end{cases} \quad (3)$$

Moreover, the equilibrium differential equations of pore ice can be presented by (Fig. 3b):

$$\begin{cases} \dfrac{\partial(\theta_i p_i)}{\partial x} + f_{six} = 0 \\ \dfrac{\partial(\theta_i p_i)}{\partial z} + f_{siz} + \theta_i \gamma_i = 0 \end{cases} \quad (4)$$

Similarly, the equilibrium differential equations of pore water can be determined as follows (Fig. 3c):

$$\begin{cases} \dfrac{\partial(\theta_w p_w)}{\partial x} + f_{swx} = 0 \\ \dfrac{\partial(\theta_w p_w)}{\partial z} + f_{swz} + \theta_w \gamma_w = 0 \end{cases} \quad (5)$$

Subsequently, by adding Eqs. (3), (4), and (5) together, the terms of interaction force can be eliminated, and the equilibrium differential equation of the frozen soil's skeleton stress can then be obtained by the following equation:

$$\begin{cases} \dfrac{\partial \sigma_x}{\partial x} + \dfrac{\partial \tau_{zx}}{\partial z} + \dfrac{1}{n}\dfrac{\partial(\theta_w p_w)}{\partial x} + \dfrac{1}{n}\dfrac{\partial(\theta_i p_i)}{\partial x} = 0 \\ \dfrac{\partial \tau_{xz}}{\partial x} + \dfrac{\partial \sigma_z}{\partial z} + \dfrac{1}{n}\dfrac{\partial(\theta_w p_w)}{\partial z} + \dfrac{1}{n}\dfrac{\partial(\theta_i p_i)}{\partial z} + \gamma_m = 0 \end{cases} \quad (6)$$

Using S_w to substitute θ_w/n in Eq. (6) to represent saturation degree of liquid water, saturation degree of ice is given as $S_i =$

$1 - S_w$. Hence, the equilibrium differential equation of the frozen soil's skeleton stress can be rewritten as follows:

$$\begin{cases} \dfrac{\partial \sigma_x}{\partial x} + \dfrac{\partial \tau_{zx}}{\partial z} + \dfrac{\partial (S_w p_w)}{\partial x} + \dfrac{\partial [(1-S_w)p_i]}{\partial x} = 0 \\ \dfrac{\partial \tau_{xz}}{\partial x} + \dfrac{\partial \sigma_z}{\partial z} + \dfrac{\partial (S_w p_w)}{\partial z} + \dfrac{\partial [(1-S_w)p_i]}{\partial z} + \gamma_m = 0 \end{cases} \quad (7)$$

Comparing Eq. (7) with the equilibrium differential equations (Eq. (1)) of total stress, the relationship between total stress, soil skeleton stress, pore ice pressure, and pore water pressure can then be obtained:

$$\sigma_t = \sigma + S_w p_w + (1-S_w)p_i \quad (8)$$

From Eq. (8), the soil skeleton stress is thus defined as:

$$\sigma = \sigma_t - S_w p_w - (1-S_w)p_i \quad (9)$$

According to the derivations above, it can be found that the soil skeleton stress results from all external forces excluding pore ice pressure and pore water pressure. Moreover, the stresses that act upon the soil skeleton, pore water, and pore ice control their own equilibrium conditions, and the soil skeleton stress is therefore referred to as the effective stress which controls the deformation and strength of the frozen soil, and it corresponds to an objective stress and has an explicitly physical meaning. Furthermore, the classical Clausius-Clapeyron equation ($p_w = \frac{v_i}{v_w} p_i + \frac{L_f T}{v_w} T_m$, e.g., Sheng et al. 2014) describing phase transition in an equilibrium thermodynamics condition is substituted into Eq. (9) to eliminate ice pressure term; the effective stress of frozen soil is then given by the following equation:

$$\sigma = \sigma_t - \frac{(\rho_w - \rho_i)S_w + \rho_i}{\rho_w} p_w + (1-S_w)\frac{L_f T \rho_i}{T_m} \quad (10)$$

where v_w and v_i are the specific volume of the water and ice, ρ_w and ρ_i stand for density of the water and ice, T represents the temperature, $T_m = 273.15$K, and L_f denotes the latent heat. If water saturation degree $S_w = 1$, then Eq. (10) transforms to Terzaghi's effective stress for saturated soil (e.g., Terzaghi 1943). A specific clay (Hu 2011) having a saturated water content of 0.24 and the dry density of 1650 kg/m³ is applied for modeling of Eq. (10). Moreover, the soil freezing characteristic of this clay ($\theta_w = \frac{\rho_d}{\rho_w} A \left(-T - \frac{\Delta v T_m}{L_f} p_w \right)^B$) considering the water pressure (Zhou and Zhou 2012) is also used for frozen soil's effective stress modeling, ρ_d denotes the dry density, $\Delta v = v_i - v_w$, and A and B are 0.099 and -0.523, respectively. Thus, if an overburden pressure σ_t pushing down on the top of the soil sample is assumed to be 200 kPa, numerical modeling shows that the effective stress of frozen soil decreases as temperature drops at a constant pore water pressure; furthermore, the effective stress decreases with the increase of

the pore water pressure at a constant temperature (Fig. 4).Therefore, both hydraulic water pressure and temperature are necessary to estimate the effective stress of the frozen soil. Interestingly, numerical results show that the negative pore water pressure not only provides cryogenic suction for water migration but also results in the consolidation of matrix skeleton since effective stress of frozen soil can exceed the overburden pressure under the effect of negative pore water pressure (Fig. 4). The consolidation phenomenon induced by the negative pore water pressure is also described and analyzed by Xia (2005). Moreover, the effective stress determines the deformation of matrix skeleton and thus causes an inevitable effect on heat and fluid transport. The strong interactions between the stress development and heat and fluid transfer make frost heave modeling an interesting task. The effective stress of the frozen soil (Eq. 10) is subsequently introduced into the mass conservation and heat transfer equations to mathematically develop a fully THM coupled frost heave model and benefit the frost heave mitigation analysis.

A fully THM coupled frost heave model

The coupled processes in the active zone

During freezing, the active zone mainly experiences the coupled thermophysical processes of heat transfer, liquid transport, and stress development. Before the appearance of
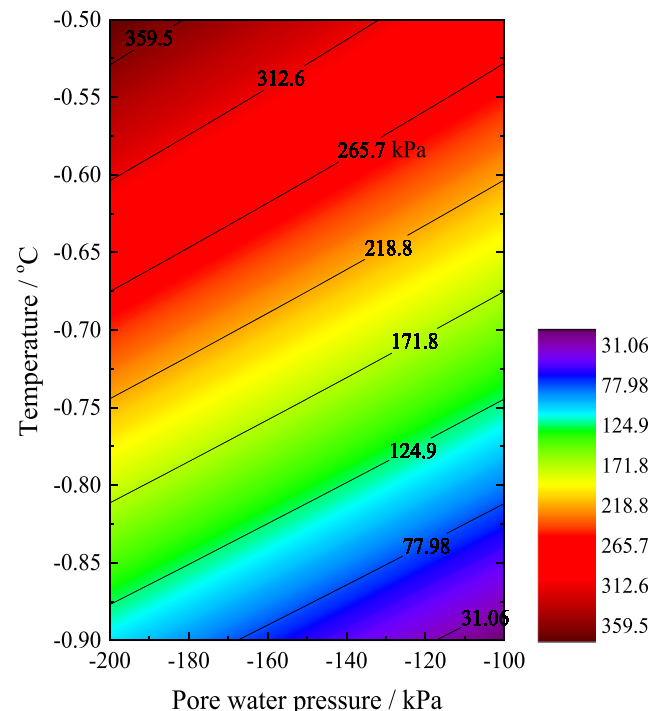
Fig. 4 The schematic of the effective stress of frozen soil under various different temperatures and pore water pressures

the ice lens during freezing, only the active zone exists in the soil sample (Fig. 5a). However, after the appearance of the latest ice lens, the bottom of the ice lens ($z = z_w$) can distinguish the freezing soil into two zones, i.e., the active zone ($z < z_w$) and the passive zone ($z > z_w$), and the frozen fringe is between freezing front ($z = z_f$) and the bottom of the ice lens (Fig. 5b). T_c, T_w, T_s, and T_f represent the cold end temperature, warm end temperature, ice lens temperature, and freezing temperature, respectively (Fig. 5b).

The governing equations used for describing the mass conservation (Eq. (11)) and heat transfer (Eq. (12)) in our previous studies (Zhou 2009; Zhou and Zhou 2012; Zhou et al. 2018) were developed and improved according to Harlan's research (1973) on heat and fluid transport in porous media:

$$\frac{\partial}{\partial z}\left(k\frac{\partial p_w}{\partial z}\right) = \frac{\partial \theta_w}{\partial t} + \frac{\rho_i}{\rho_w}\frac{\partial \theta_i}{\partial t} \tag{11}$$

$$C_v\frac{\partial T}{\partial t} = \frac{\partial}{\partial z}\left(\lambda\frac{\partial T}{\partial z}\right) + L_f\rho_i\frac{\partial \theta_i}{\partial t} \tag{12}$$

$$\theta_w = \frac{\rho_d}{\rho_w}A\left(-T-\frac{\Delta v T_m}{L_f}p_w\right)^B \tag{13}$$

where $k = K/\rho_w g$, K represents the hydraulic permeability, t is time, C_v stands for the volumetric specific heat capacity, and λ represents the thermal conductivity; Eq. (13) describes the soil freezing characteristic with considering the pore water pressure, where A and B stand for both the soil parameters.

Moreover, by assuming that both ice and matrix particles are rigid media and then considering that the effective stress of partial frozen soil is the difference between the total stress and the equivalent water pressure, the heat and fluid transport equations are improved to investigate frost heave (Zhou et al. 2018). In this section, the effective stress of frozen soil (Eq. (10)) is introduced into the heat and mass transport equations to mathematically improve a more complete governing equations for the active zone, and a fully THM coupled frost heave model is subsequently established by coupling the ice-water phase transition, segregation criterion of the ice lens, and fluid flow theory in the freezing soil.

Instead of considering a constant volume of soil skeleton, Cao et al. (2007) proposed a relationship between the deformation of soil skeleton and the effective stress if the deformation is small, and the correlation is given by:

$$\frac{\partial n}{\partial \sigma} = -\alpha \tag{14}$$

where α is the compression coefficient of the soil.

By substituting Eqs. (2), (10), and (14) into Eqs. (11) and (12), the following new equations governing the mass conservation and heat transfer can be presented as:

$$\rho_w\frac{\partial}{\partial z}\left(k\frac{\partial p_w}{\partial z}\right) = (\rho_w-\rho_i)\frac{\partial \theta_w}{\partial t} + \alpha\rho_i\left[\frac{(\rho_w-\rho_i)S_w + \rho_i}{\rho_w}\frac{\partial p_w}{\partial t} - \frac{(1-S_w)L_f\rho_i}{T_m}\frac{\partial T}{\partial t}\right] \tag{15}$$

$$C_v\frac{\partial T}{\partial t} = \frac{\partial}{\partial z}\left(\lambda\frac{\partial T}{\partial z}\right) - L_f\rho_i\frac{\partial \theta_w}{\partial t} + L_f\alpha\rho_i\left[\frac{(\rho_w-\rho_i)S_w + \rho_i}{\rho_w}\frac{\partial p_w}{\partial t} - \frac{(1-S_w)L_f\rho_i}{T_m}\frac{\partial T}{\partial t}\right] \tag{16}$$

It should be noted that the external pressure σ_t is regarded as a constant value; the term σ_t in Eqs. (15) and (16) is eliminated during derivation process because of $\partial\sigma_t/\partial t = 0$. Furthermore, Eqs. (13), (15), and (16) describing the heat and fluid flow constitute the new governing equations of the active zone.

Fig. 5 Schematic of freezing soil: (a) before the appearance of the ice lens and (b) after the appearance of the latest ice lens (revised after Konrad and Morgenstern 1980)
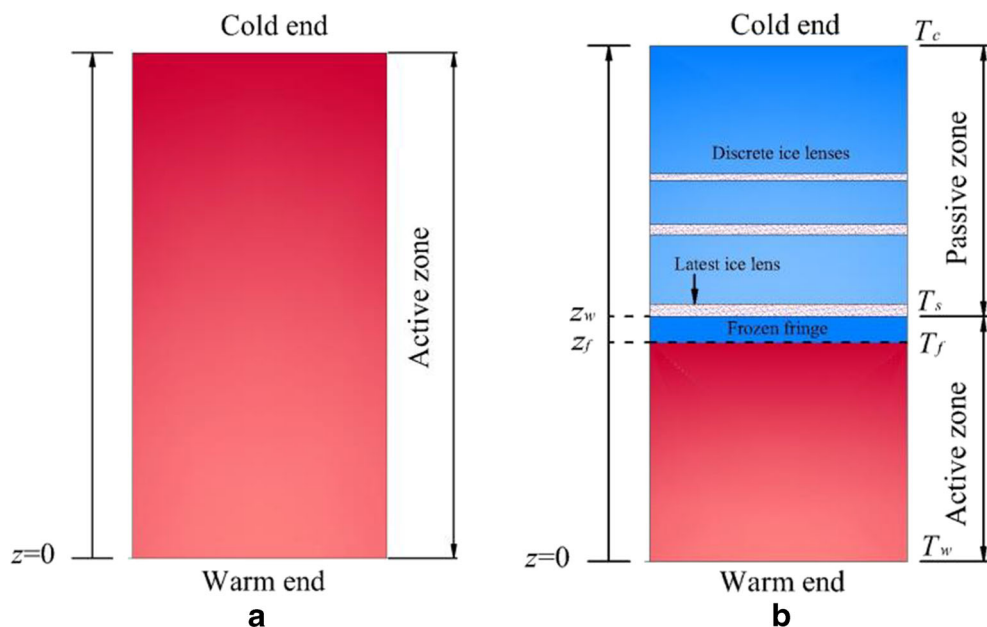
Ice lens segregation, growth, and frost heave

The formation criterion of the ice lens

The formation criterion of the ice lens in this paper is determined based on Gilpin's thermodynamic equilibrium research (1980) of ice and liquid water near a solid matrix. As the frozen fringe (intense phase transition zone) temperature decreases, the liquid water film absorbed onto the surface of solid matrix gradually becomes thinner. This physical process not only increases the liquid pressure p_{liq} but also facilitates the intrusion and approach of the ice-water interface to the surface of matrix particles and thus causes the separation of soil particles. The physical process implies that the disjoining pressure p_{liq} near the solid matrix will balance the external pressure. Therefore, the new ice lens will emerge if the disjoining pressure exceeds the external pressure. However, the tensile strength characteristics that maintain the mechanical integrity of the soil during this segregation process cannot be neglected (Gilpin 1980; Nixon 1991; Lai et al. 2017). Considering the resistances of both external pressure and tensile strength on ice lens formation, the ice lens formation criterion can be written as follows (Gilpin 1980):

$$p_{liq} \geq \sigma_t + \sigma_{tensile}^* \tag{17}$$

where $\sigma_{tensile}^*$ is the tensile strength of the soil in the frozen fringe, the disjoining pressure is $p_{liq} = (v_w p_w - v_i \sigma_{iw} \kappa - L_f T / T_m) v_i$, σ_{iw} stands for the ice-water interfacial tension, and κ represents the curvature of the ice-water interface (Zhou et al. 2018).

By coupling Eqs. (13), (15), and (16) with the boundary conditions, we can determine the pore water pressure and temperature in the active zone, then Eq. (17) can be used to calculate the disjoining pressure of p_{liq} and define the location of the newly formed ice lens and thus re-divide the active zone and the passive zone in the freezing soil.

Mageau and Morgenstern (1980) indicated that the thermal conduction is the major thermophysical process in the passive zone with insignificant phase transition and water migration:

$$C_v \frac{\partial T}{\partial t} = \frac{\partial}{\partial z}\left(\lambda \frac{\partial T}{\partial z}\right) \tag{18}$$

The growth of the ice lens

After the appearance of the newly formed ice lens, the horizontal soil-free ice lens will block the migration of water to the previous ice lens, the fluid flow driven by the cryogenic suction will feed the growth of the latest ice lens near the frozen fringe (Fig. 5), and the corresponding growth rate of the ice lens V_i can be determined by combing the principle of mass conservation:

$$V_i = \frac{\rho_w}{\rho_i} V_w\big|_{z=z_s} = -k \frac{\rho_w}{\rho_i} \frac{\partial p_w}{\partial z}\bigg|_{z=z_s} \tag{19}$$

where V_w is the migration rate of water at the base of the latest ice lens. In addition, if the overburden pressure σ_t acts upon the top of the soil, the macroscopic ice pressure at the bottom of the ice lens equals σ_t, and the cryogenic suction at the base of the ice lens can then be transformed to this form: $p_w = \frac{v_i}{v_w}\sigma_t + \frac{L_f T}{v_w} T_m$. It can be found that the pore water pressure (negative pressure) becomes less negative as the overburden pressure increases, thus causing a negative impact on the driving force for water migration. Given the intense phase transition at the base of the latest ice lens, the energy conservation equation applied to determine the temperature of the ice lens is given by:

$$\lambda_+ \frac{\partial T_+}{\partial z}\bigg|_{z=z_s} - \lambda_- \frac{\partial T_-}{\partial z}\bigg|_{z=z_s} = L_f \rho_w V_w\big|_{z=z_s} \tag{20}$$

where "+" and "−" represent the active zone and passive zone, respectively.

Frost heave in freezing soil

The thickness of the ice lens (segregation frost heave) can be obtained by integrating Eq. (19) during freezing, and the deformation caused by in situ frozen water (in situ frost heave) can be determined by considering the volume expansion caused by phase change of the local water. Additionally, the consolidation deformation incurred by the effective stress in the active zone should be calculated separately since the active zone is constituted by the frozen fringe (intense phase transformation zone) and the unfrozen soil. The formation of the ice lens at the top of the frozen fringe causes the separation of soil particles; hence, the macroscopic ice pressure p_i equals the overburden pressure σ_t. The effective stress for the frozen fringe can be simplified as follows:

$$\sigma = \sigma_t - S_w p_w - (1-S_w)\sigma_t = S_w(\sigma_t - p_w) \tag{21}$$

It can be seen from the Eq. (21) that the effective stress in the frozen fringe depends upon the saturation degree of water, which is governed by the temperature and pore water pressure at a specific position (Eq. 13). In the unfrozen zone, the water saturation degree $S_w = 1$, Eq. (21) can be transformed to the classical effective stress of saturated soil:

$$\sigma = (\sigma_t - p_w) \tag{22}$$

Equations. (21) and (22) control the consolidation deformation of the frozen fringe and the unfrozen soil, respectively. Besides the deformation in the active zone, the total frost heave can be obtained by considering the segregation frost heave and in situ frost heave.

Implementation of frost heave model

Using the finite difference method, the corresponding simulation program compiled by the Matrix Laboratory (MATLAB R2017a) software was applied to carry out the numerical simulation of frost heave. Validation of this fully coupled THM frost heave model is demonstrated through comparison of the simulated results with the freezing experiment of saturated clay. The frost heave result predicted by this model is referred to as Frost heave-I. In addition, frost heave models established by our previous studies (Zhou et al. 2018; Zhou and Zhou 2012) are also applied to simulate frost heave, and the corresponding predicted results are referred to as Frost heave-II and Frost heave-III, respectively. Zhou and Zhou's (2012) frost heave model (Frost heave-III) primarily focuses on describing the characterized growth behavior of the ice lens under the thermal-hydraulic environment. Hence, the volume expansion (in situ frost heave) caused by the phase transition of the local water is not taken into account in this model. As discussed in section 3.1, an improved frost heave model (Frost heave-II) considering the in situ frost heave and the segregation heave was proposed by coupling the deformation of soil skeleton (Zhou et al. 2018). In this paper, it should be noted that the deformation of soil skeleton is determined by the effective stress of frozen soil (section 2). Furthermore, the stress development incurred by external pressure is taken into account to present a fully coupled THM frost heave model, and the main differences between the coupled heat and fluid governing equations in each model are shown in Table 1.

Hu et al. (2011) conducted the frost heave tests with saturated clay samples having a dry density 1.65 g/cm^3 and an inner dimension of 0.1m×0.1m×0.15m. The mass fraction of clay is 0.37 and that of silt is 0.53, and the vacuum saturated water content is 0.24. The overburden pressure pushing down on the clay sample is 50 kPa, and the critical separation

pressure $\sigma_{tensile}^*$ is simplified as 25 kPa according to Nixon (1991). The compression coefficient α is 17×10^{-8} Pa^{-1}, and the soil parameters A and B used to determine the soil freezing characteristic are 0.099 and -0.523, respectively. During freezing, the constant cold end temperature is -20 °C, and warm end temperature is 12 °C, and the freezing time is set to 3480 min.

The unfrozen bulk water in the frozen fringe provides seepage conduits for water migration, and the hydraulic permeability in the frozen fringe can be determined as $K = K_{sat}(\theta_w/n)^9$ (O'Neil and Miller 1985), K_{sat} denotes the hydraulic permeability of the saturated soil (Tarnawski and Wagner 1996), and it can be presented as follows:

$$K_{sat} = 4 \times 10^{-5} \left(\frac{0.5}{1-\theta_{sat}} \right)^{1.3\left(d_g^{-0.5}+0.2\sigma_g\right)}$$
$$\times e^{(-6.88m_{cl}-3.63m_{si}-0.025)} \qquad (23)$$

where m_{cl} and m_{si} denote the mass fraction of clay and silt, respectively, and d_g and σ_g are the geometrical mean diameter and standard deviation of the matrix particles.
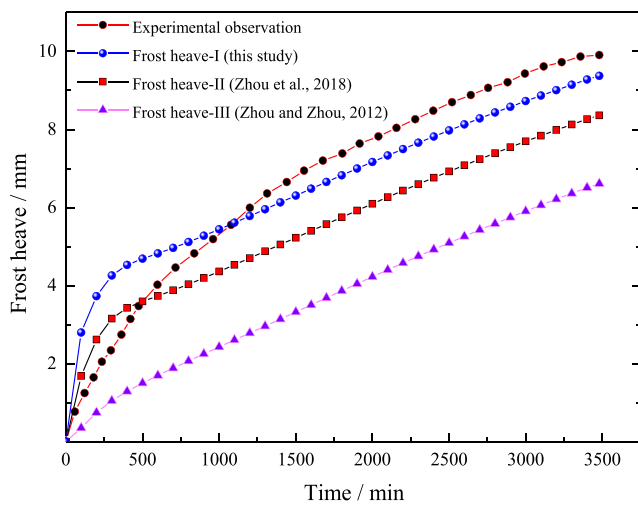
During freezing, the component contents of each phase (water and ice) vary with temperature and pore water pressure (Eq. 13) and thus cause an inevitable effect on the heat conductivity λ and heat capacity C_v of the soil. The volumetric heat conductivity and heat capacity can be written as $\lambda = \lambda_i^{\theta_i} \lambda_w^{\theta_w} \lambda_s^{\theta_s}$ and $C_v = (C_i\theta_i + C_w\theta_w + C_s\theta_s)$, respectively (e.g., Lai et al. 2014). $\theta_s = 1 - n$, and it represents the volumetric content of soil skeleton. The λ_i, λ_w, and λ_s denote the heat conductivity of the ice, water, and solid matrix, and the corresponding values are 2.32 W/(m · K), 0.58 W/(m · K), and 1.95 W/(m · K). The C_i, C_w, and C_s represent the volumetric specific heats of ice, water, and soil matrix, and the corresponding values are 2.09×10^3 kJ/(m^3·°C), 4.18×10^3 kJ/(m^3·°C), and 2.2×10^3 kJ/(m^3·°C).

The soil parameters are used to conduct numerical simulations of frost heave. The result of Frost heave-II is close to the measured result, but the result of Frost heave-I matches the measured result much better (Fig. 6). The disparity between Frost heave-I and the experimental observation is 5.4%, while the difference between Frost heave-II and the experimental

Table 1 The critical governing equations for describing the mass conservation and heat transfer in the active zone

Different models	Frost heave-I	Frost heave-II	Frost heave-III
Governing equations	$\rho_w \frac{\partial}{\partial z}\left(k\frac{\partial p_w}{\partial z}\right) = (\rho_w-\rho_i)\frac{\partial\theta_w}{\partial t}$ $+ \alpha\rho_i\left[\frac{(\rho_w-\rho_i)S_w+\rho_i}{\rho_w}\frac{\partial p_w}{\partial t}-\frac{(1-S_w)L_f\rho_i}{T_m}\frac{\partial T}{\partial t}\right]$ $C_v\frac{\partial T}{\partial t} = \frac{\partial}{\partial z}\left(\lambda\frac{\partial T}{\partial z}\right)-L_f\rho_i\frac{\partial\theta_w}{\partial t}$ $+ L_f\alpha\rho_i\left[\frac{(\rho_w-\rho_i)S_w+\rho_i}{\rho_w}\frac{\partial p_w}{\partial t}-\frac{(1-S_w)L_f\rho_i}{T_m}\frac{\partial T}{\partial t}\right]$	$\rho_w\frac{\partial}{\partial z}\left(k\frac{\partial p_w}{\partial z}\right) = (\rho_w-\rho_i)\frac{\partial\theta_w}{\partial t}+\alpha\rho_i\frac{\partial p_w}{\partial t}$ $C_v\frac{\partial T}{\partial t} = \frac{\partial}{\partial z}\left(\lambda\frac{\partial T}{\partial z}\right)+L_f\alpha\rho_i\frac{\partial p_w}{\partial t}-L_f\rho_i\frac{\partial\theta_w}{\partial t}$	$\frac{\partial}{\partial z}\left(k\frac{\partial p_w}{\partial z}\right) = \frac{\partial\theta_w}{\partial t}+\frac{\rho_i}{\rho_w}\frac{\partial\theta_i}{\partial t}$ $C_v\frac{\partial T}{\partial t} = \frac{\partial}{\partial z}\left(\lambda\frac{\partial T}{\partial z}\right)+L_f\rho_i\frac{\partial\theta_i}{\partial t}$

Fig. 6 Comparison of frost heave between experimental observation and numerical simulation

observation is 15.6%. The improved governing equations provide a more accurate quantitative evaluation of the thermal and hydraulic state of the freezing soil, and this will benefit thermal parameters calculation and further facilitate and improve the frost heave prediction. The disparity between the predicted result (Frost heave-III) and the measured result increases to 33.2%. At the initial stage of freezing, the predicted result of Frost heave-III is smaller than that of Frost heave-I and II, and this implies that the in situ frost heave caused by the phase transition of local water is necessary for frost heave prediction (Fig. 6). Furthermore, both results of Frost heave-I and Frost heave-II present a similar trend, and the heaving rate decreases with time (Fig. 6). Actually, the thermal gradient induced water pressure gradient drives the continuous flow of water into the frozen fringe. The cold end temperature propagates rapidly toward the warm end at the initiation of freezing due to thermal diffusion; the decreasing rate of temperature subsequently slows down (Fig. 7a and b). The propagation of cold temperature gradually decreases and stabilizes the temperature gradient. Additionally, the stable ice crystals formed in the frozen fringe cause pore blocking and thus reduce the seepage conduits and affect the flow of liquid in the freezing soil. Both of the two physical processes decrease the velocity of water migration and frost heave. Furthermore, the comparison between the results of Frost heave-I and the measurement verifies the fully THM coupled frost heave model, and it is subsequently applied for a specific study of frost heave mitigation.

Frost heave mitigation

In order to mitigate the detrimental effects of frost heave and to find an optimal scheme of FSPR for Gongbei undersea

tunnel project of Hong Kong-Zhuhai-Macao Bridge, Hu et al. (2017) proposed a technical concept and method ("freeze-up, anti-weakening, frost heave control") for frost heave mitigation. This method can effectively limit and control the thickness of frozen soil by circulating a higher temperature brine in the limiting tube. The monitoring results from an actual construction indicate that this method can effectively control the development of the freezing soil and ensure the quality of the undersea tunnel project. This innovation of the freezing technique will provide engineering experience and a method for large-section engineering construction (e.g., tunneling and shaft sinking) under complex geological and geographical environments for water proofing and strengthening soil. In order to reduce frost heave, some chemical and physical methods (e.g., salinization treatment (Sarsembayeva and Collins 2017) and engineered structure for frost heave prevention (Li et al. 2012; Zhao et al. 2020)) can be used to mitigate frost heave. It is noted that the cold end temperature is still a critical parameter that can be controlled for the artificial freezing process if the construction environment and conditions are difficult to change for a specific engineering project. The boundary temperature dominates the temperature gradient and freezing rate in the soil and affects the crystallization, phase transformation, and water migration process, resulting in a difference in distribution and growth of discrete ice lens. Zhou's research team (Zhou 1999; Zhou et al. 2006; Hu et al. 2011) applied the intermittent freezing method to investigate the physical process of frost heave and found that this method can mitigate frost heave efficiently, whereas the corresponding mitigation mechanism still needs to be explored and addressed.

In order to observe and discuss the effects of intermittent freezing on frost heave, a sinusoidal function (Eq. (24)) is used as an example at the top of the soil to simulate the intermittent temperature (-10 to -20 °C) and to show the mitigation effect caused by intermittent freezing (Fig. 8), and the newly established THM frost heave model in section 3 is applied to investigate and explore frost heave mitigation and its physical process.

$$T_c(t) = -15 + 5sin\left(\frac{\pi}{15}t\right) \tag{24}$$

where the amplitude and the period of intermittent freezing are 5 °C and 30 min, respectively.

The same soil parameters and frost heave model established in this study (section 3.3) are applied to simulate frost heave under intermittent freezing. The corresponding frost heave result is referred to as the Frost heave-IV, and the Frost heave-I obtained under the continuous freezing (section 3.3) is used to compare with frost heave under the intermittent freezing. Numerical results show that intermittent freezing can significantly reduce frost heave, the simulation
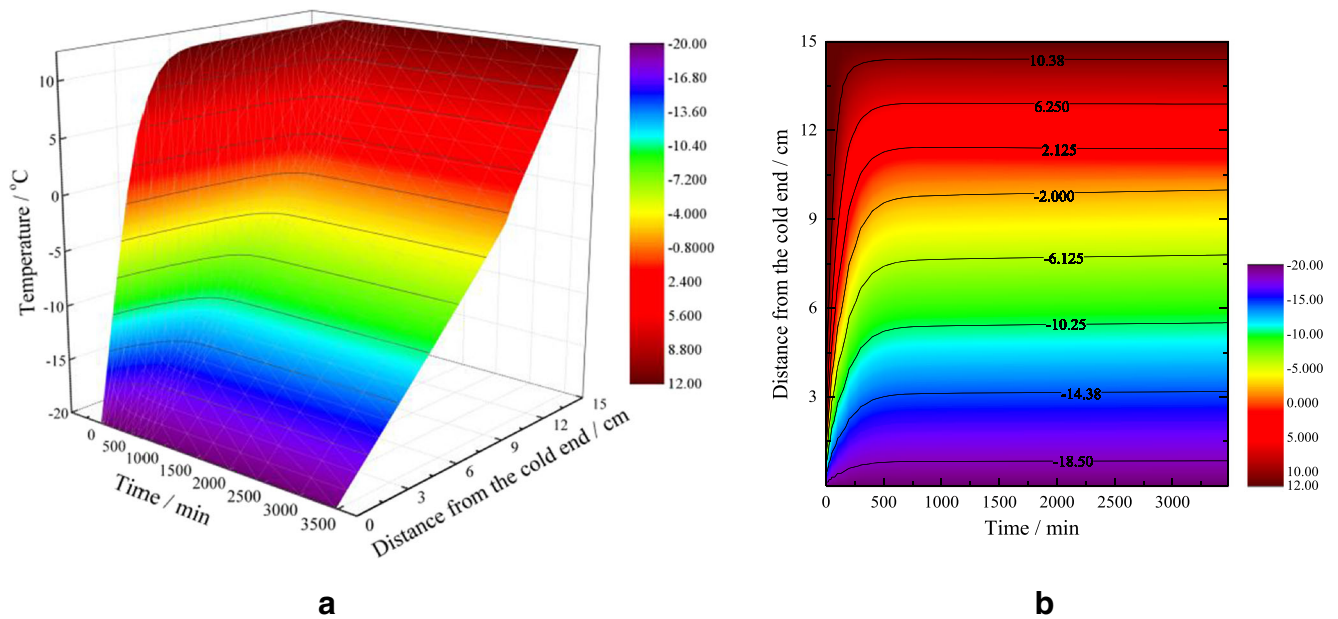
Fig. 7 The temperature distribution and variation in different times (Frost heave-I): (**a**) temperature distribution during freezing (5 to 3480 minutes) and (**b**) temperature variation during freezing (5 to 3480 minutes)

results of frost heave under the intermittent freezing and continuous freezing are 7.64 mm and 9.38 mm, respectively (Fig. 9a). Moreover, the frost heave ratio (frost heave divided by frost depth) as the normalized data are 7.84% and 8.77%, respectively; this implies that the intermittent freezing can not only mitigate frost heave but also limit the frost susceptibility of the soil. By selecting the frost heave data from 1950 to 2250 min, we find that the patterns of frost heave under the two freezing modes present a different trend (Fig. 9b). The pattern of frost heave under the condition of Frost heave-IV increases intermittently rather than continuously, and an obvious step pattern of frost heave is presented under intermittent freezing (Fig. 9b). The interesting macro-behavior of frost
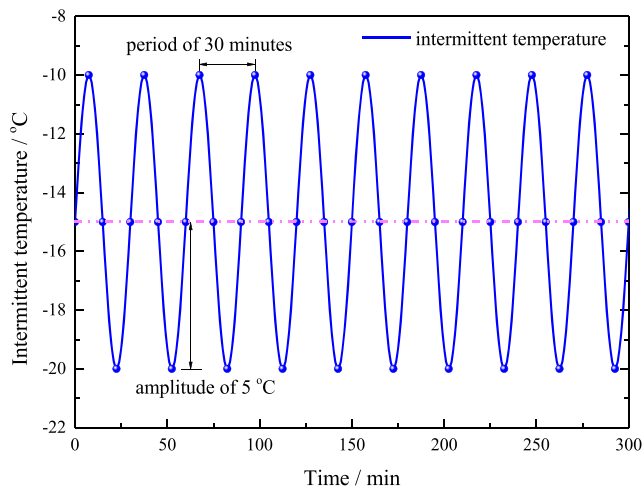
heave demonstrates that intermittent freezing can significantly mitigate the continuity growth of the ice lens and thus decrease frost heave.

During freezing, the intense phase transition in the frozen fringe provides the driving force for water migration, and further exploration on the physical properties of the frozen fringe and the growth mechanism of ice lens will potentially enable a better understanding of frost heave mitigation and facilitate further development of the artificial freezing technique. During intermittent freezing, the frost heave rate significantly decreases with the narrowing of the frozen fringe, and it increases with a thickening frozen fringe (Fig. 10). Thus, the geometrical structure of the frozen fringe has an inevitable impact on frost heave. The narrowing of the frozen fringe reflects the upward movement of the freezing front, and the corresponding temperature of the ice lens increases during this physical process and decreases the driving force for water migration, resulting in a limitation of ice lens growth and frost heave (Fig. 10). The intermittent increase of frost heave implies that the existence of the frozen fringe is a necessary condition for the stable and rapid growth of the ice lens (Fig. 10). Moreover, taking account of force balance between the thermomolecular force, hydrodynamic force, and overburden, Rempel et al. (2004) proposed a relationship between the growth rate of the ice lens and its boundary position. The growth characteristic shows that the heave rate of the ice lens depends strongly on the ice lens boundary position and decreases when the freezing front approaches the ice lens. Therefore, when the engineering geological conditions have been determined, using the flexible cold end temperature to control
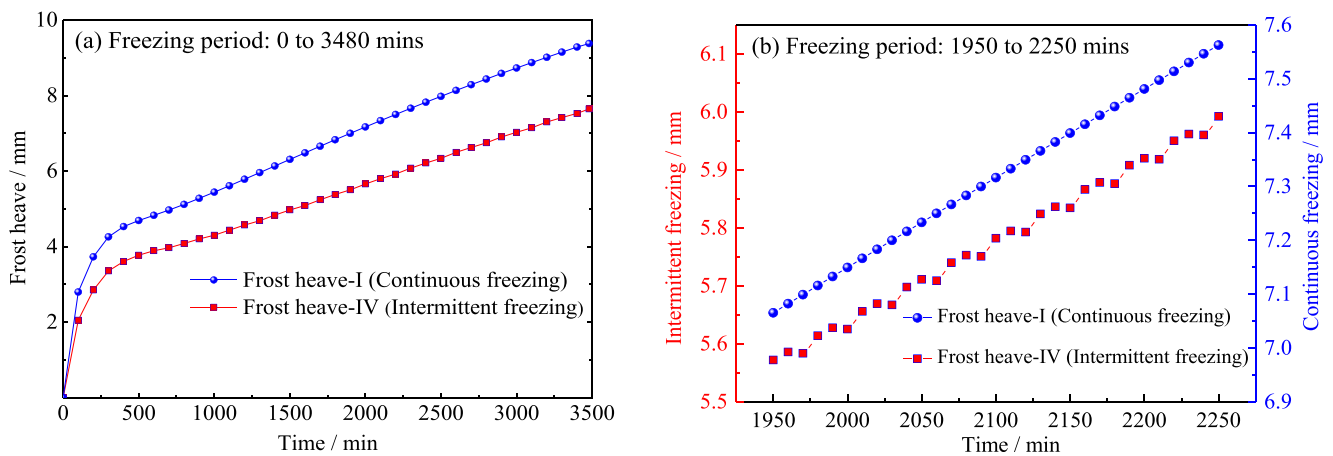

Fig. 8 The profile of the intermittent temperature

Fig. 9 Frost heave under the intermittent freezing and continuous freezing: (**a**) freezing period: 0 to 3480 min and (**b**) freezing period: 1950 to 2250 min

the thickness of the frozen fringe will effectively decrease the growth of the ice lens and mitigate frost heave in an actual freezing engineering construction. In the construction of the Gongbei tunnel, a high-temperature brine circulated limiting tube was applied to induce the backward movement of freezing front and to control the development of freezing soil (Hu et al. 2017), which limits the propagation of the freezing front and reduces the in situ frost heave, which reduces the thickness of the frozen fringe and thus results in reduced frost heave.

In conclusion, the presence of the frozen fringe is significant for hydrodynamics and thermodynamics physical processes in freezing soil and thus in enabling a stable growth of the ice lens. Therefore, using the new THM coupled frost heave model, the intermittent freezing is evaluated and analyzed as an effective artificial freezing method. Numerical results show that intermittent freezing causes the narrowing of the frozen fringe and thus benefits frost heave mitigation.

Conclusions

(1) Taking the soil skeleton, pore ice, and pore water as the independent bodies to conduct the mechanical equilibrium analysis, the pore water pressure and temperature-dependent effective stress of frozen soil are proposed in this paper by considering the multiphase interactions (ice-water-mineral). Considering the effect of soil skeleton deformation on heat and fluid transport, the governing equations describing mass conservation and heat transfer are improved. By coupling the ice-water phase transition, the formation and growth of the discrete ice lenses, and the thermal conduction in the passive zone, a fully coupled THM frost heave model is subsequently established.

(2) The fully coupled THM frost heave model provides a quantitative method to predict frost heave and to analyze frost heave mitigation under the intermittent freezing

Fig. 10 The schematic of mitigation mechanism of frost heave
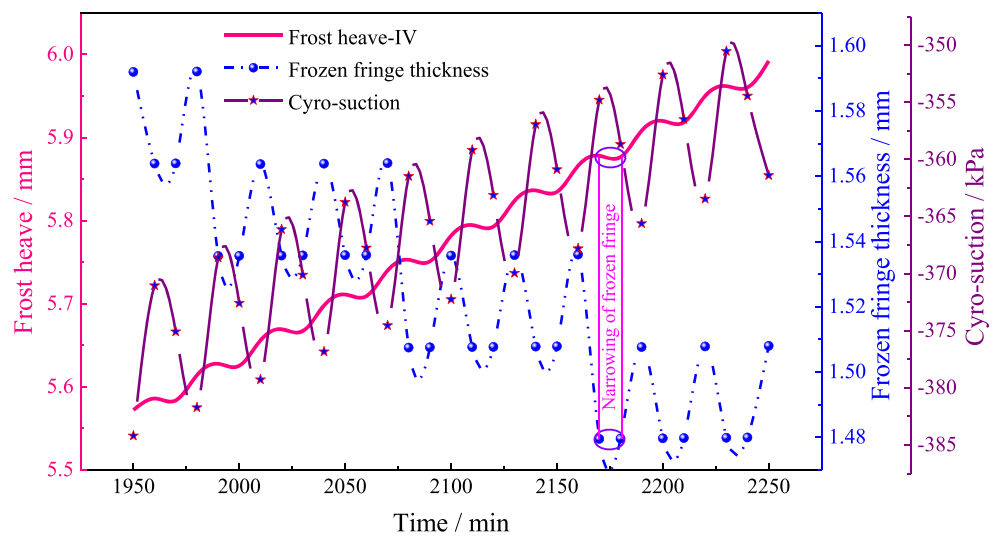
condition. Numerical simulations show that intermittent freezing results in a characterized step pattern of frost heave instead of a continuous increasing pattern of frost heave under a continuous freezing. Furthermore, the intermittent freezing can significantly mitigate frost heave and inhibit the potential frost susceptibility of freezing soil.

(3) During intermittent freezing, the simulated results indicate that the cryogenic structure of the frozen fringe is significant for the ice lens growth, and the intermittent freezing induced upward movement of the freezing front results in the narrowing of the frozen fringe and thus decreases the growth rate of the ice lens and enables the mitigation of frost heave. Accordingly, when the latest ice lens is formed, a meaningful artificial freezing technique which can induce the backward movement of freezing front will mitigate frost heave and engineering damages in cold regions.

References

Azmatch TF, Sego DC, Arenson LU, Biggar KW (2012a) New ice lens initiation condition for frost heave in fine-grained soils. Cold Reg Sci Technol 82:8–13

Azmatch TF, Sego DC, Arenson LU, Biggar KW (2012b) Using soil freezing characteristic curve to estimate the hydraulic conductivity function of partially frozen soil. Cold Reg Sci Technol 83-84:103–109

Black PB, Tice AR (1989) Comparison of soil freezing and soil water curve data for Windsor sandy loam. Water Resour Res 25(10):2205–2210

Bronfenbrener L, Bronfenbrener R (2010) Modeling frost heave in freezing soils. Cold Reg Sci Technol 61:43–64

Cao H, Liu S, Jiang F, Liu J (2007) The theoretical study of frost heave for saturated granular soil-numerical simulation of 1-D ice segregating model based on equilibrium of force and phase. Chin J Theoretic Appl Mechan 30(6):848–857 **(In Chinese)**

Dash JG, Fu H, Wettlaufer JS (1995) The premelting of ice and its environmental consequences. Rep Prog Phys 58(1):115–167

Everett DH (1961) The thermodynamics of soil moisture. Trans Faraday Soc 57:1541–1551

Gilpin RR (1980) A model for the prediction of ice lensing and frost heave in soils. Water Resour Res 16(5):918–930

Harlan RL (1973) Analysis of coupled heat-fluid transport in partially frozen soil. Water Resour Res 9(5):1314–1323

Hansson K, Šimůnek J, Mizoguchi M, Lundin LC, van Genuchten MT (2004) Water flow and heat transport in frozen soil: numerical solution and freeze-thaw applications. Vadose Zone J 3:693–704

Hu K (2011) Development of separated ice model coupled heat and mass transfer in freezing soils. PhD. Thesis (In Chinese). China University of Mining and Technology, Xuzhou

Hu K, Zhou G, Zhang Q, Li T (2011) Influence of temperature amplitudes and time intervals on frost heave. Indust Construct 41(3):86–90 **(In Chinese)**

Hu X, Deng S (2016) Ground freezing application of intake installing construction of an underwater tunnel. Procedia Eng 165:633–640

Hu X, Deng S, Ren H (2017) In situ test study on freezing scheme of freeze-sealing pipe roof applied to the Gongbei tunnel in the Hong Kong-Zhuhai-Macau bridge. Appl Sci 7(1):27

Hu X, Deng S, Wang Y (2018a) Test investigation on mechanical behavior of steel pipe-frozen soil composite structure based on freeze-sealing pipe roof applied to Gongbei tunnel. Tunn Undergr Sp Tech 79:346–355

Hu X, Fang T, Chen J, Ren H, Guo W (2018b) A large-scale physical model test on frozen status in freeze-sealing pipe roof method for tunnel construction. Tunn Undergr Sp Tech 72:55–63

Ji Y, Zhou G, Zhou Y, Hall MR, Zhao X, Mo P (2018) A separate-ice based solution for frost heaving-induced pressure during coupled thermal-hydro-mechanical processes in freezing soils. Cold Reg Sci Technol 147:22–33

Ji Y, Zhou G, Hall MR (2019) Frost heave and frost heaving-induced pressure under various restraints and thermal gradients during the coupled thermal–hydro processes in freezing soil. B Eng Geol Environ 78:3671–3683

Koopmans RWR, Miller RD (1966) Soil freezing and soil water characteristic curves. Soil Sci Soc Am J 30(6):680–685

Konrad JM, Morgenstern NR (1980) A mechanistic theory of ice lens formation in fine-grained soils. Can Geotech J 17(4):473–486

Lackner R, Amon A, Lagger H (2005) Artificial ground freezing of fully saturated soil: thermal problem. J Eng Mech 131:211–220

Li Z, Liu S, Feng Y, Liu K, Zhang C (2012) Numerical study on the effect of frost heave prevention with different canal lining structures in seasonally frozen ground regions. Cold Reg Sci Technol 85:242–249

Lai Y, Pei W, Zhang M, Zhou J (2014) Study on theory model of hydro-thermal–mechanical interaction process in saturated freezing silty soil. Int J Heat Mass Transf 78:805–819

Lai Y, Wu D, Zhang M (2017) Crystallization deformation of a saline soil during freezing and thawing processes. Appl Therm Eng 120:463–473

Li S, Zhang M, Pei W, Lai Y (2018) Experimental and numerical simulations on heat-water-mechanics interaction mechanism in a freezing soil. Appl Therm Eng 132:209–220

Lyu C, Sun Q, Zhang W (2019) Effects of NaCl concentration on thermal conductivity of clay with cooling. B Eng Geol Environ 79:1449–1459

Miller RD (1972) Freezing and heaving of saturated and unsaturated soils. Highw Res Rec 393:1–11

Mageau DW, Morgenstern NR (1980) Observations on moisture migration in frozen soils. Can Geotech J 17(17):54–60

Nixon JF (1991) Discrete ice lens theory for frost heave in soil. Can Geotech J 28(6):843–859

O'Neil K, Miller RD (1985) Exploration of a rigid ice model of frost heave. Water Resour Res 21(3):281–296

Rempel AW, Wettlaufer JS, Worster MG (2004) Premelting dynamics in a continuum model of frost heave. J Fluid Mech 498:227–244

Rempel AW (2007) Formation of ice lenses and frost heave. J Geophys Res 112:F02S21

Spaans EJA, Baker JM (1996) The soil freezing characteristic: its measurement and similarity to the soil moisture characteristic. Soil Sci Soc Am J 60:13–19

Shao L, Zheng G, Guo X, Liu G (2014) Principle of effective stress for unsaturated soils. Proceeding of the 6th international conference on unsaturated soils, Sydney, Australia, pp 239–245

Sheng D, Zhang S, Niu F, Cheng G (2014) A potential new frost heave mechanism in high-speed railway embankments. Géotechnique 64(2):144–154

Shao L, Guo X, Liu S, Zheng G (2017) Effective stress and equilibrium equation for soil mechanics. CRC Press, Boca Raton

Sarsembayeva A, Collins PEF (2017) Evaluation of frost heave and moisture/chemical migration mechanisms in highway subsoil using a laboratory simulation method. Cold Reg Sci Technol 133:26–35

Terzaghi K (1943) Theoretical soil mechanics. John Wiley, New York

Tarnawski VR, Wagner B (1996) On the prediction of hydraulic conductivity of frozen soils. Can Geotech J 33(1):176–180

Wang Y, Wang D, Ma W, Wen Z, Chen S, Xu X (2018) Laboratory observation and analysis of frost heave progression in clay from the Qinghai-Tibet plateau. Appl Therm Eng 131:381–389

Xia D (2005) Frost heave (MSc thesis). University of Alberta, Edmonton

Zhou G (1999) Analysis of mechanism of restraining soil freezing swelling by using intermission method. J China Univ Min Technol 128(5):413–416 **(In Chinese)**

Zhou J, Zhou G, Ma W, Wang J, Zhou Y, Ji S (2006) Experimental research on controlling frost heave of artificial frozen soil with intermission freezing method. J China Univ Min Technol 35(6):708–712 **(In Chinese)**

Zhou Y (2009) Study on frost heave model and frost heave control of frozen soil. PhD. Thesis (In Chinese). China University of Mining and Technology, Xuzhou

Zhou Y, Zhou G (2012) Intermittent freezing mode to reduce frost heave in freezing soils–experiments and mechanism analysis. Can Geotech J 49(6):686–693

Zhang S, Sheng D, Zhao G, Niu F, He Z (2016) Analysis of frost heave mechanisms in a high-speed railway embankment. Can Geotech J 53(3):520–529

Zhang X, Zhang M, Lu J, Pei W, Yan Z (2017) Effect of hydro-thermal behavior on the frost heave of a saturated silty clay under different applied pressures. Appl Therm Eng 117:462–467

Zhou G, Zhou Y, Hu K, Wang Y, Shang X (2018) Separate-ice frost heave model for one-dimensional soil freezing process. Acta Geotech 13(1):207–217

Zhao R, Zhang S, Gao W, He J, Wang J, Jin D, Nan B (2019) Factors effecting the freeze thaw process in soils and reduction in damage due to frosting with reinforcement: a review. B Eng Geol Environ 78:5001–5010

Zhang B, Wang H, Ye Y, Tao J, Zhang L, Shi L (2019) Potential hazards to a tunnel caused by adjacent reservoir impoundment. B Eng Geol Environ 78:397–415

Zhao R, Zhang S, He J, Gao W, Jin D, Xie L (2020) Experimental study on freezing and thawing deformation of geogrid-reinforced silty clay structure. B Eng Geol Environ 79:2883–2892